Towards a better understanding of the color shift of effect coatings by densely sampled spectral BRDF measurement

Alejandro Ferrero[1]*[a], Berta Bernad[a], Joaquín Campos[a], Francisco M. Martínez-Verdú[b], Esther Perales[b], Ivo van der Lans[c] and Eric Kirchner[c]

[a]Instituto de Óptica, Consejo Superior de Investigaciones Científicas (CSIC), c/Serrano 144, Madrid 28006, Spain; [b]Department of Optics, Pharmacology and Anatomy, University of Alicante, Carretera de San Vicente del Raspeig s/n 03690, Alicante, Spain; [c]AkzoNobel Automotive & Aerospace Coatings, Color Research Group, Rijksstraatweg 31, 2171 AJ Sassenheim, The Netherlands

ABSTRACT

To completely characterize the color of effect coatings, the spectral BRDF should be measured for a large number of illumination/detection geometries. This is possible with the GEFE, the gonio-spectrophotometer developed at *Instituto de Óptica* in CSIC (IO-CSIC). Twenty-four effect coating samples were prepared by AkzoNobel, containing metallic and/or interference flake pigments. The spectral BRDF of all samples was measured by GEFE using a normalized procedure under 448 different geometries. The results are presented in two-dimensional a*-b* diagrams and in three-dimensional CIELAB diagrams to show the color travel. Four different descriptors were used to quantify the color travel of these samples. We show that for many samples and geometries, the resulting colors fall outside the color gamut of a typical display. It was found that the reflection data do not vary considerably at reciprocal geometries, allowing a reduction of geometries to be done. Finally, we show that for 3D rendering applications, the reflection data from BRDF can be strongly reduced. For example, we show that using the concept of flake-based parameters it is possible to only use in-plane geometries. The resulting rendered images were shown to be accurate enough for rendering on displays.

Keywords: Special effect coatings, spectral BRDF, interference pigments, metallic coatings, rendering, spectrophotometry

1. INTRODUCTION

The color of effect coatings depends strongly on the illumination and detection geometries, giving them a very appealing appearance. As a consequence, these coatings have become very popular in the automotive industry and in other applications such as cosmetics and security inks. Effect coatings consist of a transparent medium containing traditional absorption pigments and flake-shaped effect pigments. To completely characterize the color of these coatings under any illuminant and for any illumination/detection geometry, their spectral Bidirectional Reflectance Distribution Function (BRDF) should be measured for a large number of measurement geometries, thus providing all information required to characterize the color shift.

In this article, we will show the results by two-dimensional a*-b* diagrams and by three-dimensional CIELAB plots. The color travel that is obvious from these diagrams is quantified by a number of recently introduced descriptors. We will investigate to what extent the various colors fall inside the color gamut of a typical display.

Next, we will show that the reflection data do not vary considerably at reciprocal geometries. The results are used to argue that a strong reduction in reflection data should be possible for characterizing effect coatings. One method for data reduction is to use only in-plane data. We will investigate the validity of that approach for 3D rendering applications.

[1] *alejandro.ferrero@csic.es

Measuring, Modeling, and Reproducing Material Appearance, edited by Maria V. Ortiz Segovia, Philipp Urban, Jan P. Allebach, Proc. of SPIE-IS&T Electronic Imaging, SPIE Vol. 9018, 90180K
© 2014 SPIE-IS&T · CCC code: 0277-786X/14/$18 · doi: 10.1117/12.2036726

Downloaded From: http://proceedings.spiedigitallibrary.org/ on 04/25/2014 Terms of Use: http://spiedl.org/terms

2. METHODS AND MATERIALS

2.1 Instrumentation and measurement

GEFE, the gonio-spectrophotometer developed at the *Instituto de Óptica* in CSIC (IO-CSIC) [1] allows the spectral BRDF to be measured at any geometry, including out-of-plane and retro-reflection angles. The spectral BRDF was measured by GEFE following a normalized procedure. We selected polar angles with respect to the sample normal to vary from 0° to 70° in steps of 10°, both for illumination (θ_{ill}) and detection (θ_{det}) directions. The azimuthal angle of the detection direction (ϕ_{det}) was varied from 0° to 180° in steps of 30°, assuming symmetry with respect to the incident angle. The resulting BRDF contains $8\times8\times7 = 448$ different geometries. The azimuthal angle of illumination (ϕ_{ill}) was not varied, since preliminary measurements showed that anisotropy was negligible under azimuthal rotations of the samples.

Table 1. Samples prepared by AkzoNobel for this work.

Sample name	Classification	Effect pigment
01	Blue, very fine metallic	Silberline Sparkle Silver
02	Blue, less fine metallic	Silberline Sparkle Silver
03	Blue, coarser metallic	Silberline Sparkle Silver
04	Blue, very coarse metallic	Silberline Sparkle Silver
05	Green, very fine metallic	Silberline Sparkle Silver
06	Green, less fine metallic	Silberline Sparkle Silver
07	Green, coarser metallic	Silberline Sparkle Silver
08	Green, very coarse metallic	Silberline Sparkle Silver
09	Pearl with significant color travel	Iriodin combination pigment
10	Pearl with fine coarseness	Xirallic Crystal Silver
11	Pearl with color travel from blue to green	Colorstream Viola Phantasy
12	Pearl with color travel green-blue-purple	Chromaflair Green Purple
13	Pearl, also with large color travel	Chromaflair Green Purple
14	Pearl. Color travel green to yellow	Chromaflair Gold Silver
15	Pearl. Similar to sample 14	Chromaflair Gold Silver
16	Pearl. Similar to sample 14	Chromaflair Gold Silver
17	Grey metallic, very dark	Silberline Sparkle Silver, Eckart Stapa Metallux, Exterior Mearlin Fine Blue
18	Grey metallic, less dark	Silberline Sparkle Silver
19	Grey metallic, lighter	Silberline Sparkle Silver
20	Grey metallic, very light	Silberline Stapa Metallux
21	Very bright orange pearl	Merck Meoxal Wahiba
22	Bright red non-metallic	Paliocrom Gold and conventional mica pearls.
23	Bright orange non-metallic	Paliocrom Gold (and also a metallic Silberline Stapa Metallux)
24	Light green non-metallic	Paliocrom Gold (and also a metallic Silberline Stapa Metallux)

2.2 Samples

Twenty-four effect coating samples were prepared by AkzoNobel and characterized by using the GEFE instrument. These samples contain metallic and/or interference pigments, as shown in Table 1. The samples can be classified into two groups:

(1) Metallic coatings. We included textures varying from very fine to very coarse.

(2) Interference coatings with a varying degree of color travel as depending on illumination/detection angle. These samples included for example Iriodin®, Xirallic®, Colorstream® and Meoxal® pigments from Merck and Chromaflair® pigments from JDSU.

Downloaded From: http://proceedings.spiedigitallibrary.org/ on 04/25/2014 Terms of Use: http://spiedl.org/terms

2.3 Representation of data

The results are presented in two-dimensional a*-b* diagrams and three-dimensional CIELAB diagrams to show the color travel. For the sake of clarity, only in-plane and non-specular measurements are shown in the 2D plots as usually. The points in these plots were connected by lines corresponding to the well-known interference lines. These are lines for which the aspecular angle remains constant, i.e. the angle between detection and the specular direction. Interference lines have been discussed in great detail before [2][3]. The measurement points are also connected by lines representing so-called absorption lines. This is a concept recently introduced [4]. It refers to measurement geometries that keep the bistatic angle constant, i.e. the angle between detection and illumination direction.

3. TWO DIMENSIONAL a*,b*-DIAGRAMS

The resulting measurement data for a selection of samples are plotted in a*,b*-diagrams in Figures 1 and 2. As mentioned above, the plots show solid red lines for interference lines, connected by blue discontinuous lines for absorption lines. Figures 1a and 1b refer to samples 01 and 05. These are both metallic samples with a very fine texture. Sample 20, the data of which are shown in Figure 1c, is also a metallic sample. As an illustration of the change in characteristics for other types of effect pigments, Figures 1d – 1f and Figure 2 show data for some of the other samples. Below, we will go into more detail for non-metallic effect coatings.

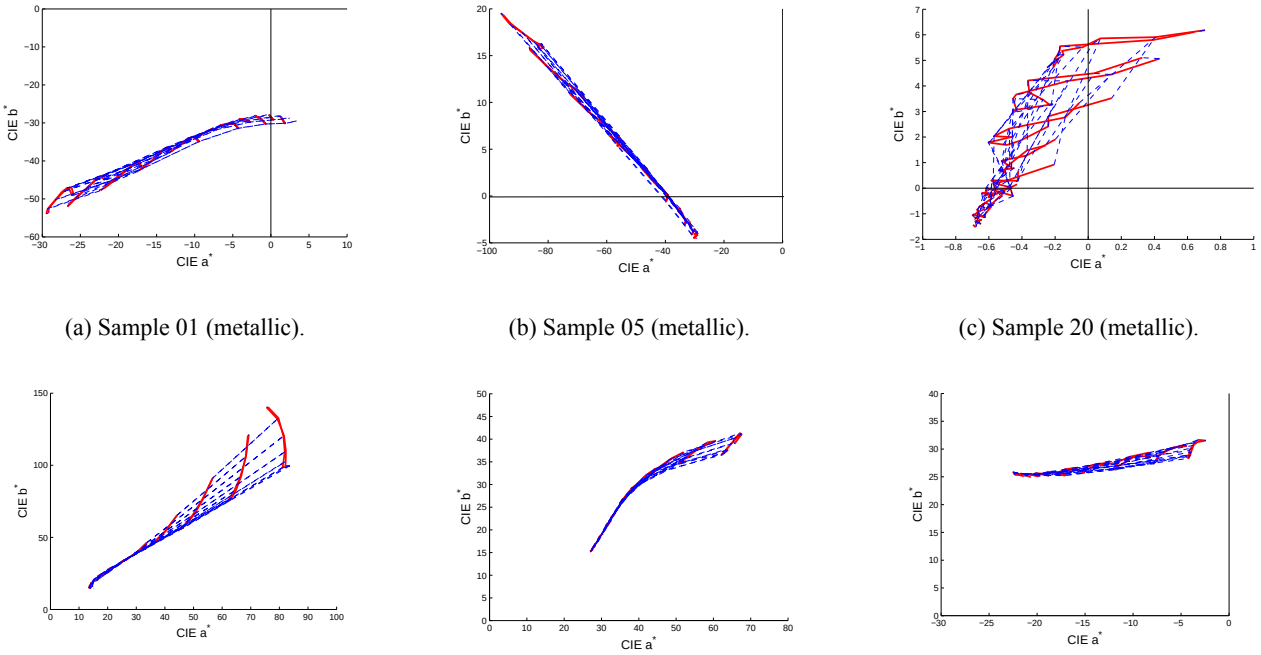

(a) Sample 01 (metallic). (b) Sample 05 (metallic). (c) Sample 20 (metallic).

(d) Sample 21 (non-metallic). (e) Sample 22 (non-metallic). (f) Sample 24 (non-metallic).

Figure 1. Measured color representation in a*,b*-diagrams of samples 01, 05, 20, 21, 22 and 24. Red lines refer to interference lines, whereas blue lines refer to absorption lines.

3.1 Quantifying the color shift

For the metallic samples shown in Figure 1a and 1b, a very characteristic behavior is found in the a*-b* plots. Although the color category for these samples is very different (blue and green, respectively) the characteristic one-dimensional character of the interference lines for metallic samples is easily recognized. Sample 20 is also a metallic coating, and Figure 1c shows a similar behavior (notice the scale in this plot).

Downloaded From: http://proceedings.spiedigitallibrary.org/ on 04/25/2014 Terms of Use: http://spiedl.org/terms

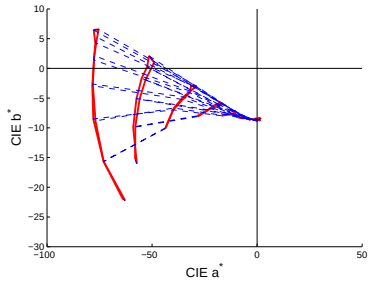

(a) Sample 09 (Mica-Combination pigment).

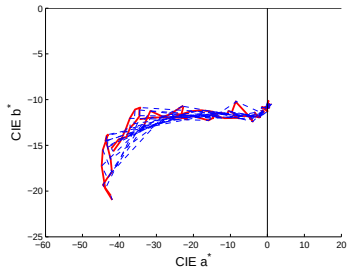

(b) Sample 10 (Xirallic Crystal Silver).

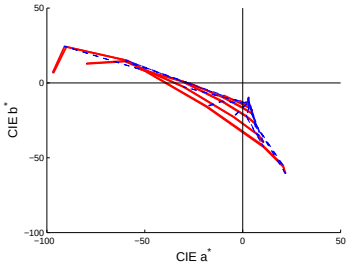

(c) Sample 11 (Colorstream Viola Phantasy).

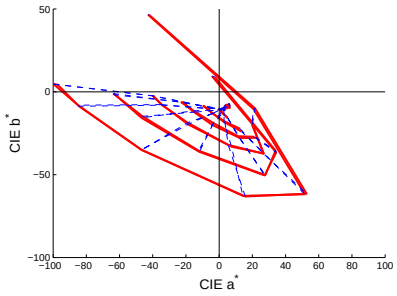

(d) Sample 12 (Chromaflair Green Purple).

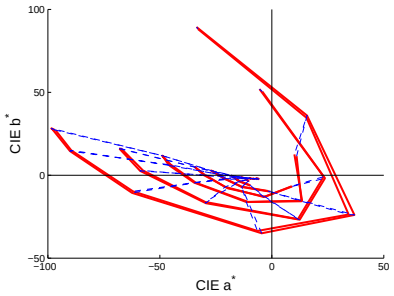

(e) Sample 13 (Chromaflair Green Purple).

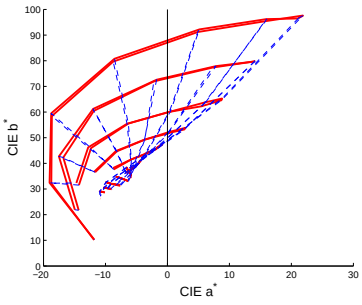

(f) Sample 14 (Chromaflair Gold Silver).

Figure 2. Measured color representation in a*,b*-diagrams of samples 09, 10, 11, 12, 13 and 14. Red lines refer to interference lines, whereas blue lines refer to absorption lines.

The most important feature of special effect coatings is their strong color shift, as illustrated in Fig. 2. This shift is well characterized by the dense-sampled measurements of spectral BRDF that we have presented in this work. However, for many applications a more simple numeric quantity is needed to quantify the color shift. A number of different candidates were introduced in a recent article by some of the present co-authors [4]:

1) Total hue angle variation: the maximum variation in hue angle along the interference line with aspecular angle θ_{asp}=10º. The capacity of this descriptor to quantify hue shift and to discriminate between special effect coatings and other coatings is clearly shown in Figure 3a, where the descriptor values for all measured samples are displayed.

2) Chroma variation: the maximum variation of chroma along the absorption line with bistatic angle θ_{bi}=10º. This absorption line is the one which cuts the interference line with aspecular angle θ_{asp}=10º at an extreme in Figures 2a, c, d, e and f. Samples 20 and 24 show clearly the lowest chroma variation in Figure 3b.

3) Absorption chroma: on the absorption line with bistatic angle θ_{bi}=10º, it is the chroma at the highest aspecular angle, when scattering from absorption pigment prevails over reflection from interference pigments. Also here, Sample 20 shows the lowest value of this descriptor in Figure 3c. However, in this case sample 24 is shown to be a special case with the highest absorption but with very low chroma variation (cf. Figure 2f).

4) Contribution from absorption pigments (C_A): from smaller to larger angles, it is the minimum aspecular angle θ_{asp} at which the hue angle is not constant anymore along the length of the absorption line. It describes how large the overall contribution to color is from the scattering from absorption pigments. In the case of special effect coatings, the lower its value, the higher the contribution to color from these pigments. Sample 11 presents the lowest value (Figure 3d), which means that color due to absorption pigments is already contributing at a smaller value for the aspecular angle than for the other special-effect samples.

Downloaded From: http://proceedings.spiedigitallibrary.org/ on 04/25/2014 Terms of Use: http://spiedl.org/terms

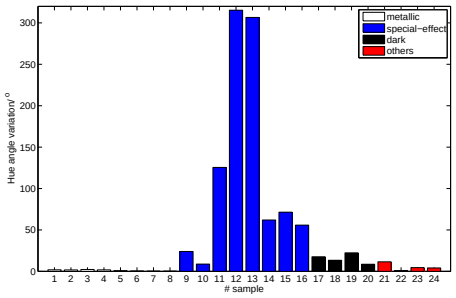

(a) Total hue angle variation.

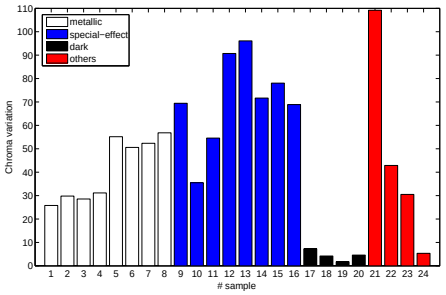

(b) Chroma variation.

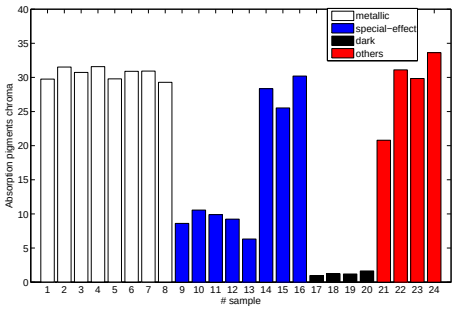

(c) Absorption chroma.

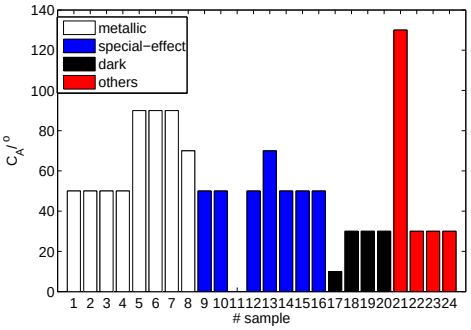

(d) Contribution from absorption pigments.

Figure 3. Calculated values for measured samples of descriptors proposed to characterize the color shift of effect and special-effect coatings.

3.2 Comparing spectral BRDF at reciprocal geometries

The results that we have obtained for the many measurement geometries investigated for this work allow us to identify redundant geometries. These are sets of geometries with identical spectral BRDF. If Helmholtz reciprocity principle would be fulfilled, then one of each pair of geometries 1 and 2 with $(\theta_{ill,1}, \phi_{ill,1}) = (\theta_{det,2}, \phi_{det,2})$ and $(\theta_{det,1}, \phi_{det,1}) = (\theta_{ill,2}, \phi_{ill,2})$ would be redundant. Geometries 1 and 2 for which $\theta_{ill,1} = \theta_{det,2}$; $\theta_{det,1} = \theta_{ill,2}$; and $|\phi_{det,1}-\phi_{ill,1}|=|\phi_{det,2}-\phi_{ill,2}|$ will be called reciprocal geometries here. One of such a pair of geometries is redundant if these samples are isotropic under an azimuthal rotation of the sample, and, obviously, if Helmholtz reciprocity principle is fulfilled.

We compared the color of 84 pairs of reciprocal geometries, excluding those in the incident plane (Helmholtz-reciprocal geometries in our data), and those with ϕ_{det}-ϕ_{ill}=30º (occluded geometries to some extent for some cases). The resulting average color differences and the associated standard deviations between reciprocal geometries for the measured samples are shown in Figure 4. Except for four effect coating samples and for sample 10 (Xirallic), the average color difference is smaller than 1. In only one case, sample 04, these values are larger than 2. From this comparison we conclude that generally Helmholtz's reciprocity principle is fulfilled by effect coatings. This indicates also that the samples investigated here are isotropic with respect to azimuthal rotation of the samples. This result shows that the number of geometries required to characterize effect coating samples can be notably reduced by taking into account redundant pairs of geometries. One example of such data reduction is to only use in-plane geometries, as further discussed below. Other examples of data reduction are discussed in a forthcoming paper [5].

Downloaded From: http://proceedings.spiedigitallibrary.org/ on 04/25/2014 Terms of Use: http://spiedl.org/terms

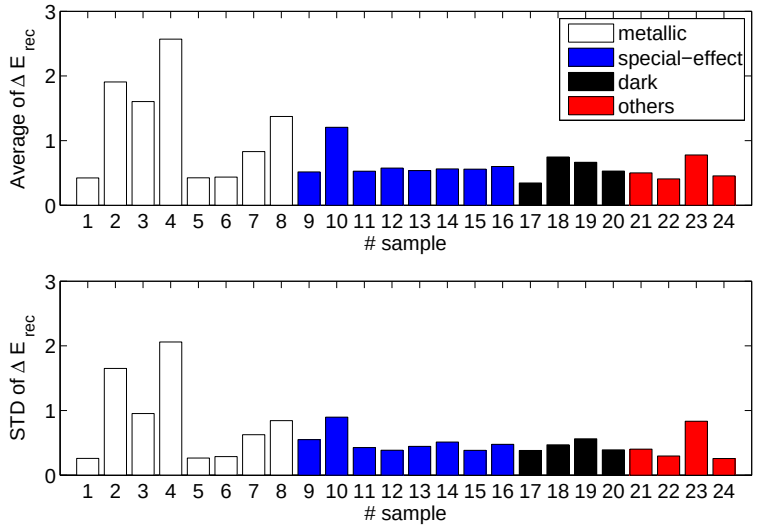

Figure 4. Average color difference (top) and standard deviation (bottom) between reciprocal geometries for the measured samples.

4. THREE DIMENSIONAL CIELAB DIAGRAMS

The colors that were measured for the samples were plotted in CIELAB color space in order to be compared with the color gamut of a typical display. Based on the spectral BRDF measurement data, CIELAB values were calculated by taking the CIE 1964-XYZ standard observer and the D65 illuminant into account. The color gamut of the display was obtained by assuming the sRGB color space following the international standard IEC 61966-2-1:1999.

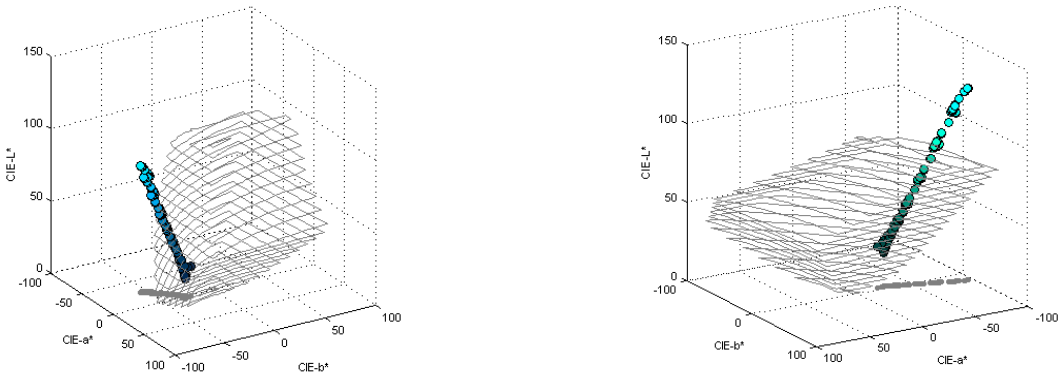

(a) Sample 01 (b) Sample 05

Figure 5. Three-dimensional CIELAB diagrams for (a) Sample 01 and (b) Sample 05.

In Figure 5-7, only in-plane and non-specular measurements are shown. The color dots refer to the samples at different measurement geometries. The colored points in these figures correspond to the real color samples as calculated by transforming XYZ tristimulus values into sRGB values. In addition, in these figures grey points indicate the projection on the CIE a*-b* diagram. Also the color gamut of the display is plotted by constant lightness profiles (from L* = 0 to L* = 100 in steps of 5) for better visualization.

Figure 5 shows the color gamut of two metallic samples, sample 01 and 05. The lightness and chroma shift along the measurement geometries are easily recognized. We note that for high lightness values the color samples are outside the

Downloaded From: http://proceedings.spiedigitallibrary.org/ on 04/25/2014 Terms of Use: http://spiedl.org/terms

color gamut of a typical display. This is the case for lightness values larger than L* = 100 in Figure 5b. But this is also shown for a case with L* < 100 in Figure 5a: in that case the sample has more colorfulness than what is covered by the sRGB color gamut.

The results for an achromatic metallic grey panel (sample 20) are shown in Figure 6a. In this case, the very light color obviously lies outside the display color gamut. For some measurement geometries, this panel has L* = 140. Figure 6b shows a very bright orange color. Many colors associated with different measurement geometries clearly fall outside the color gamut of a typical display, since the chroma of this sample is larger than the maximum chroma achieved by the display. It would be interesting to compare the present set of measurement data with the Rösch-MacAdam color solid under D65, as was done for other samples in Ref. [6].

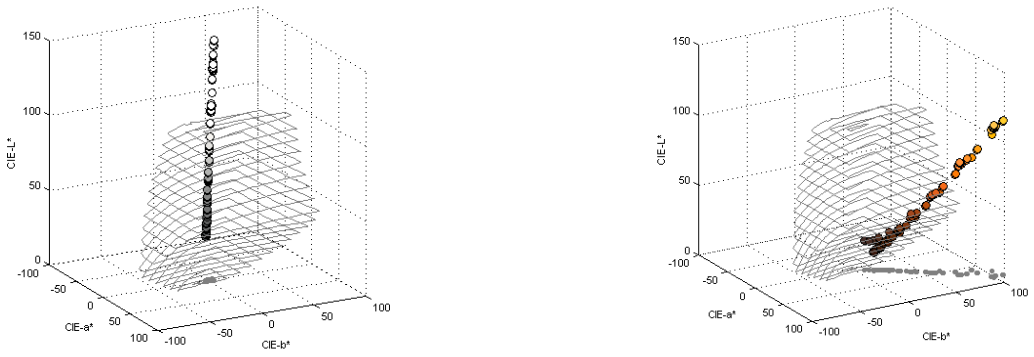

(a) Sample 20 (b) Sample 21

Figure 6. Three-dimensional CIELAB diagrams for (a) Sample 20 and (b) Sample 21.

Finally, Figure 7 shows the color gamut of samples 11 and 12. Both samples are special effect coatings, and the resulting lightness and chroma shift is clearly recognized in Figure 7. As in the previous examples, the colors associated with different measurement geometries are outside the color gamut of a typical display.

Based on our results, for a more faithful reproduction of goniochromatic materials on electronic displays one may need e.g. gamut-mapping algorithms, or new extended RGB color spaces. Alternatively, multi-primaries displays may be needed.

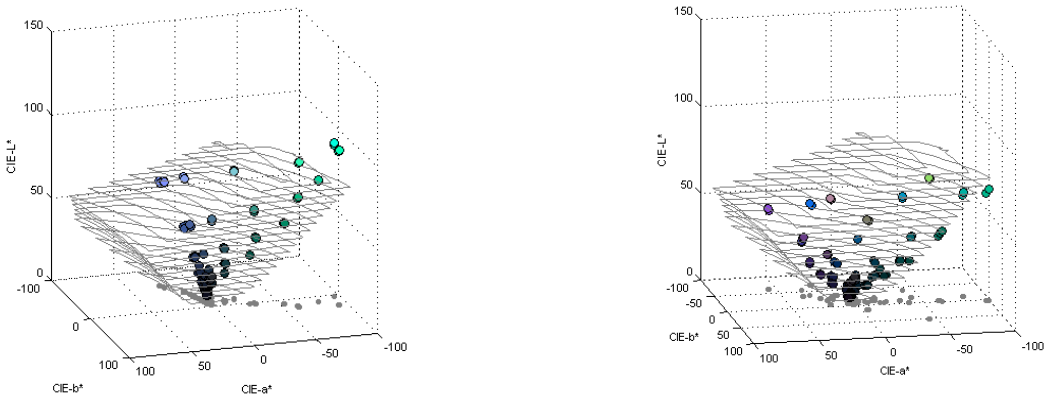

(a) Sample 11 (b) Sample 12

Figure 7. Three-dimensional CIELAB diagrams for (a) Sample 11 and (b) Sample 12.

Downloaded From: http://proceedings.spiedigitallibrary.org/ on 04/25/2014 Terms of Use: http://spiedl.org/terms

5. RECONSTRUCTING BRDF'S FROM IN-PLANE DATA

Measuring a complete BRDF at a uniform grid of angular coordinates is time consuming. To reduce time and costs, a more crude angular resolution could be used for all angular parameters, i.e. the polar angles of illumination θ_{ill} and detection θ_{det}, and the azimuthal angles of illumination ϕ_{ill} and detection ϕ_{det}. However, for many applications cruder angular sampling is not acceptable. For example, for 3D rendering applications such sampling easily results in visible artifacts.

In a recent publication, an alternative angular coordinate system was introduced that is based on a new physical approach to the optics of effect coatings. With these so-called flake-based parameters, one can calculate sets of measurement geometries that from the point of view of optics are expected to yield virtually identical reflection data [3]. Based in this approach, some of the authors have proposed that it is possible to completely characterize the spectral BRDF of a sample using a small number of properly selected in-plane geometries [7].

Here, we apply the technique of flake-based parameters to 3D rendering in the following way. From the full BRDFs that were generated for the samples mentioned in section 2, we throw away all data that do not relate to in-plane measurements. From the in-plane data (which all have $\phi_{ill} = 0°$ and $\phi_{det} = 0°$ or 180°) we can generate reconstructed reflection curves for out-of-plane geometries (which have ϕ_{det} unequal to 0° or 180°) by ensuring that the values for the flake-based parameters of the out-of-plane geometry are equal to those for an in-plane geometry. The calculations to do so can be carried out numerically by using the equations given in Ref. [3]. Alternatively, one could use a set of inverse equations that will be published soon [5].

We tested the validity of this method, which reconstructs a full BRDF from a strongly reduced set of in-plane geometries, for 3D rendering purposes as follows. We produced 3D rendering images for a simple square panel viewed under an oblique angle, based on either the reduced BRDF or the full BRDF. Using Matlab, we define a square panel with sides of equal length and pixel count. The angular position of a point light source and the detector are defined by angles θ_{ill}, ϕ_{ill}, θ_{det} and ϕ_{det} (all with respect to the normal to the panel center) and they are placed at identical distances, as shown in Figure 8. For each pixel j in the rendered image, we calculated the corresponding values of $\theta_{ill,j}$, $\phi_{ill,j}$, $\theta_{det,j}$ and $\phi_{det,j}$ with respect to the detector and the light source. For this set of parameter values, we retrieved the reflection data for the full BRDF. We used well-known interpolation techniques such as tri-linear and cubic interpolated uniform grid methods to calculate the reflection data for any given geometry, based on the full-BRDF set of reflection data.

Apart from that, we also calculated the flake-based parameters corresponding to $\theta_{ill,j}$, $\phi_{ill,j}$, $\theta_{det,j}$ and $\phi_{det,j}$, and identified in-plane geometries with the same values for the flake-based parameters. The reflection data for this in-plane geometry was found by interpolating the data from a subset of BRDF data that referred to in-plane geometries. Both the reflection data from the full BRDF and from the in-plane subset of BRDF are then converted into CIEXYZ and CIELAB, and into RGB values to produce the rendered image. The subset of BRDF geometries with in-plane geometries contains 120 geometries (θ_{ill}=0°, 10°…70°, θ_{det}=-70°, -60°…+70°, ϕ_{det}=0°).

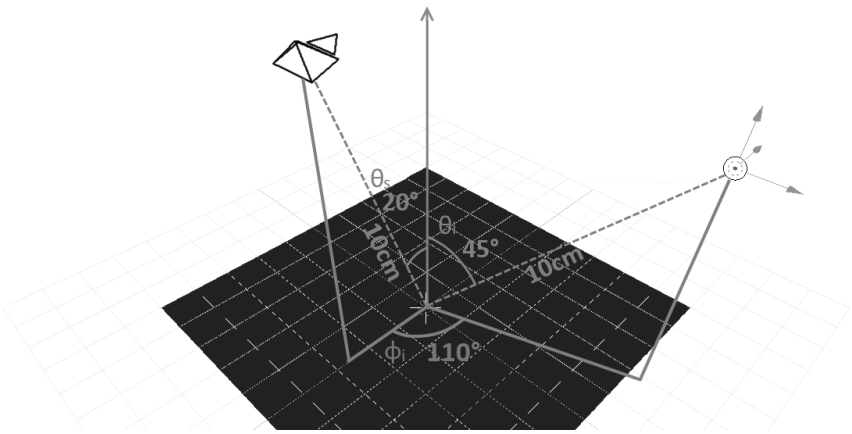

Figure 8. Geometry specification for the 3D rendering of a square panel. Detector is at $\theta_{det} = 20°$ and $\phi_{det} = 0°$. Light source is placed at $\theta_{ill} = 45°$ and $\phi_{ill} = 110°$. Detector and light source have an equal distance of 10 cm from the panel's center. Each side of the panel is 10 cm.

Downloaded From: http://proceedings.spiedigitallibrary.org/ on 04/25/2014 Terms of Use: http://spiedl.org/terms

The resulting 3D renderings are shown in Figure 9, for three samples: Metallic sample 08 (top row of images), metallic sample 20 (center row) and pearlescent sample 12 (bottom row). In the left column, the rendering images are shown as based on the full BRDF measured for each sample. In the center column, the rendering is based on the reduced set of BRDF data, including only in-plane geometries.

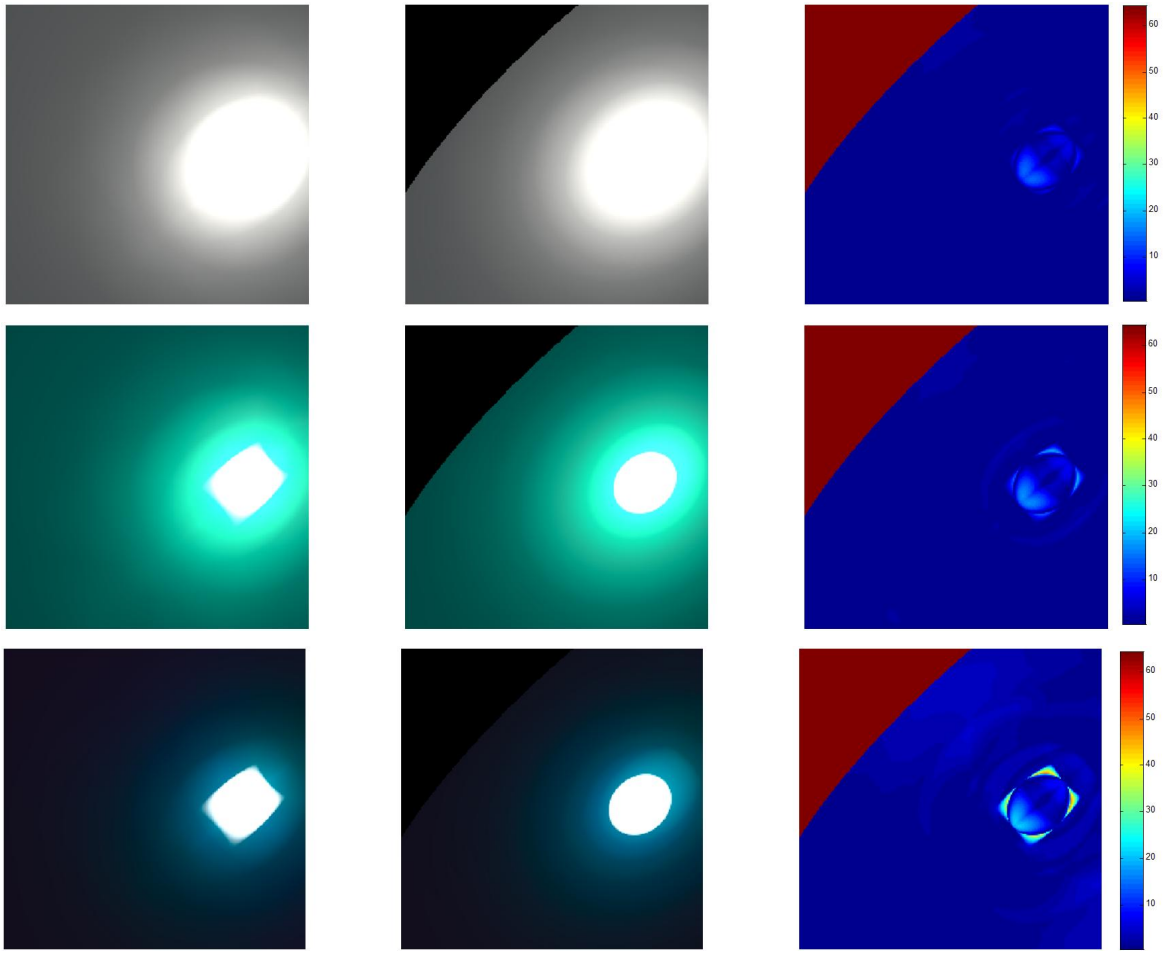

Figure 9. Results for 3D rendering of the scene shown in Figure 8, for (top images) Sample 08, (middle images) Sample 20, and (bottom images) Sample 12. The rendering is based on (left images) the full BRDF and on (center images) reduced in-plane subset of BRDF. The column on the right shows the resulting color differences dE_{CMC} between the full-BRDF and the reduced-BRDF renderings.

The images at the center-left and bottom-left, which are based on the full-BRDF, show a mirror-image of the light source that is clearly distorted in shape. The reason for this is that close the gloss angle, the set of data from the full-BRDF shows a relatively crude angular resolution in the azimuthal angle of detection ϕ_{det}. This resolution was 30°, as mentioned before. So even though we use a BRDF containing 448 different geometries, we see that for 3D rendering purposes the angular resolution may not be fine enough, when standard interpolation techniques are used. In the center column of Figure 9, such distortions do not occur because for calculating rendering images on the reduced set of BRDF geometries, interpolation based on flake-based parameters produces a more smooth interpolation.

Generally, the rendered images from the full-BRDF and those from the reduced subset of the BRDF look very similar. For the purpose of 3D rendering, these images indicate that by utilizing only in-plane reflection data one can well reconstruct the full BRDF as far as 3D rendering applications are concerned. For the reduced set of the BRDF we found that a problem arose in the top-left corners of the images (see center column in Figure 9). In these corners, the

Downloaded From: http://proceedings.spiedigitallibrary.org/ on 04/25/2014 Terms of Use: http://spiedl.org/terms

corresponding out-of-plane geometries could successfully be converted into in-plane geometries using the concept of flake-based parameter. However, the resulting in-plane geometries turned out to have values for the polar angle of illumination θ_{ill} and/or detection θ_{det} that exceed 70°. Since no geometries with such values had been included in the full BRDF set of data, the corresponding reflection data could not be generated. Obviously, this is not a fundamental problem of the method, but it must be considered when selecting geometries for measuring the BRDF. Alternatively, one could extrapolate BRDF data to values of θ_{ill}, $\theta_{det} > 70°$.

The right column of Figure 9 shows the calculated color difference dEcmc(1.5:1) (based on a 10° observer) between the two sets of reflection data that we use for the 3D rendering, i.e. the reflection data based on the full BRDF and those based on the reduced subset of BRDF. Apart from the area with the distorted mirror image of the light source and the area with lacking in-plane data, as mentioned above, all calculated color differences remain smaller than 5 units. These errors, which are the result of the interpolation techniques that we use both for the full-BRDF and the reduced-BRDF case, are small enough to be invisible on typical computer displays. Our results therefore indicate that the proposed reconstruction of BRDF data based on a reduced subset of in-plane data works well for 3D rendering purposes.

6. CONCLUSIONS

For twenty-four effect coating samples we measured the BRDF, under 448 different geometries. The reflection data obtained for the samples was compared to the color gamut of typical displays. We showed that for many samples and for many geometries, the resulting colors fall outside the color-gamut of an electronic display. This occurred both in terms of high lightness values, but also for highly saturated colors.

We evaluated four descriptors that were recently introduced to quantify color shift, and found that these parameters describe different aspects of the color shifts. We also found that the reflection data do not vary considerably at reciprocal geometries, so it should be possible to reduce the number of geometries needed to characterize these samples.

A general method for data-reduction will be discussed in a forthcoming paper [5]. Here, we tested a method that was recently proposed to reduce the amount of BRDF data needed for 3D rendering [3]. Based on flake based parameters, only in-plane is needed to reconstruct the full BRDF. By rendering a 3D scene for three types of material and using either the full BRDF or the reduced subset of BRDF data, the accuracy obtained with this method was shown to be sufficient for typical 3D rendering applications.

7. ACKNOWLEDGEMENTS

Authors are grateful to “Plan Nacional de Física” for funding this work FIS2010-19756-E, to CSIC’s JAE Program and ”European Social Fund” for awarding us a research grant. This study was also supported by the Spanish Ministry of Economy and Competitiveness under the grant DPI2011-30090-C02-02 and the European Union.

REFERENCES

[1] Rabal, A. M., Ferrero, A., Campos, J., Fontecha, J. L., Pons, A., Rubiño, A. M. and Corróns, A. (2012). “Automatic gonio-spectrophotometer for the absolute measurement of the spectral BRDF at in-and out-of-plane and retroreflection geometries,” Metrologia, 49(3), 213-223 (2012).
[2] Cramer, W.R. and Gabel, P.W. “Effektvolles messen,” Farbe und Lack 107, 42–48 (2001).
[3] Kirchner, E.J.J. and Cramer, W.R., “Making sense of measurement geometries for multi-angle spectrophotometers,” Col Res Appl 37, 186-198 (2012).
[4] Ferrero, A., Perales, E., Rabal, A.M., Campos, J., Martínez-Verdú, F.M., Chorro, E. and Pons, A., “Color representation and interpretation of special effect coatings,” J Opt Soc Am A 2014 (*accepted*).
[5] Kirchner, E.J.J. and Ferrero, A., “Isochromatic lines as generalization of the Helmholtz reciprocity principle specifically for effect coatings,” J Opt Soc Am A (*to be submitted*).

Downloaded From: http://proceedings.spiedigitallibrary.org/ on 04/25/2014 Terms of Use: http://spiedl.org/terms

[6] Perales, E., Chorro, E., Cramer, W.R. and Martínez-Verdú, F.M., "Analysis of the colorimetric properties of goniochromatic colors using the MacAdam limits under different light sources," Appl Opt 50, 5271-5278 (2011).
[7] Ferrero, A., Rabal, A., Campos, J., Martínez-Verdú, F., Chorro, E., Perales, E., Pons A and Hernanz, M.L., "Spectral BRDF-based determination of proper measurement geometries to characterize color shift of special effect coatings," J Opt Soc Am A 30(2), 206-214 (2013).

Downloaded From: http://proceedings.spiedigitallibrary.org/ on 04/25/2014 Terms of Use: http://spiedl.org/terms